THE COMMUNITY EARTH SYSTEM MODEL (CESM) LARGE ENSEMBLE PROJECT

A Community Resource for Studying Climate Change in the Presence of Internal Climate Variability

BY J. E. KAY, C. DESER, A. PHILLIPS, A. MAI, C. HANNAY, G. STRAND, J. M. ARBLASTER, S. C. BATES, G. DANABASOGLU, J. EDWARDS, M. HOLLAND, P. KUSHNER, J.-F. LAMARQUE, D. LAWRENCE, K. LINDSAY, A. MIDDLETON, E. MUNOZ, R. NEALE, K. OLESON, L. POLVANI, AND M. VERTENSTEIN

By simulating climate trajectories over the period 1920–2100 multiple times with small atmospheric initialization differences, but using the same model and external forcing, this community project provides a comprehensive resource for studying climate change in the presence of internal climate variability.

Internal climate variability, by which we mean unforced climate variability intrinsic to a given climate state, arises from atmospheric, oceanic, land, and cryospheric processes and their coupled interactions. Internal climate variability is known to have important effects on climate change projections, especially at regional spatial scales and subdecadal time scales (e.g., Hawkins and Sutton 2009; Deser et al. 2014). Nevertheless, internal climate variability is often underappreciated and confused with model error [e.g., as discussed in Tebaldi et al. (2011)]. Why? In general, modeling centers contribute a small number of realizations to international climate change projection assessments [e.g., phase 5 of the Coupled Model

AFFILIATIONS: KAY—Department of Atmospheric and Oceanic Sciences, University of Colorado Boulder, Boulder, Colorado; DESER, PHILLIPS, MAI, HANNAY, STRAND, BATES, DANABASOGLU, EDWARDS, HOLLAND, LAMARQUE, LAWRENCE, LINDSAY, MIDDLETON, MUNOZ, NEALE, OLESON, and VERTENSTEIN—Climate and Global Dynamics Division, National Center for Atmospheric Research, Boulder, Colorado; ARBLASTER—Climate and Global Dynamics Division, National Center for Atmospheric Research, Boulder, Colorado, and Bureau of Meteorology, Melbourne, Victoria, Australia; KUSHNER—Department of Physics, University of Toronto, Toronto, Ontario, Canada; POLVANI—Department of Applied Physics and Applied Math, and Department of Earth and Environmental Sciences, Columbia University, New York, New York

CORRESPONDING AUTHOR: Jennifer E. Kay, Cooperative Institute for Research in Environmental Sciences, University of Colorado Boulder, 216 UCB, Boulder, CO 80309
E-mail: jennifer.e.kay@colorado.edu

The abstract for this article can be found in this issue, following the table of contents.

DOI:10.1175/BAMS-D-13-00255.1

In final form 25 September 2014

Intercomparison Project (CMIP5; Taylor et al. 2012)]. As a result, model error and internal climate variability are difficult, and at times impossible, to disentangle. In response, we designed the Community Earth System Model Large Ensemble (CESM-LE) with the explicit goal of enabling assessment of recent past and near-future climate change (1920–2100) in the presence of internal climate variability (Table 1). Two companion, 1000+-yr-long, preindustrial, control simulations (fully coupled, prognostic atmosphere and land only) enable assessment of internal climate variability in the absence of climate change.

Unlike perturbed physics ensembles (e.g., Murphy et al. 2004) or multimodel ensembles of opportunity (e.g., CMIP5), all 30 CESM-LE members use the same model and the same external forcing. Each CESM-LE ensemble member has a unique climate trajectory because of small round-off level differences in their atmospheric initial conditions. Simply put, the CESM-LE ensemble spread results from internally generated climate variability alone.

The influence of small, initial condition differences on climate projections in the CESM-LE parallels initial condition impacts on weather forecasts (Lorenz 1963). After initial condition memory is lost, which occurs within weeks in the atmosphere, each ensemble member evolves chaotically, affected by atmospheric circulation fluctuations characteristic of a random, stochastic process (e.g., Lorenz 1963; Deser et al. 2012b). As we will show, internal climate variability has a substantial influence on climate trajectories, an influence that merits further investigation, comparison with available observations, and communication. Evaluating the realism of internal climate variability simulated by the CESM-LE is challenging, especially on decadal time scales, but vital (e.g., Goddard et al. 2013), especially given differences in model variability (e.g., Knutson et al. 2013). Model biases can degrade the realism of simulated internal variability and forced climate responses and we therefore encourage users of the CESM-LE to understand relevant model biases and their potential ramifications.

The CESM-LE builds upon previous large ensemble projects (e.g., Roeckner et al. 2003; Deser et al. 2012b; Mudryk et al. 2014; Fischer et al. 2013) with its (i) comprehensive, community-selected, freely available, and easily accessed outputs; (ii) well-documented experimental design that enables future contributions of additional ensemble members and off-shoot experiments; (iii) simulation length from the early twentieth century to the late twenty-first century; and (iv) long (1000+ yr) companion preindustrial control simulations. Given these attributes, the CESM-LE experiment uniquely enables a diverse community to assess the influence of internal climate variability and forced climate change on the climate system.

The purpose of this article is two-fold. First, we document the CESM-LE experimental design, including model version, control run and ensemble generation, external forcing, and outputs saved. Second, we provide thought-provoking examples and promising directions for use of the CESM-LE by climate scientists and stakeholders.

EXPERIMENTAL DESIGN. All CESM-LE simulations use a single CMIP5 coupled climate model: the Community Earth System Model, version 1, with the Community Atmosphere Model, version 5 [CESM1(CAM5); Hurrell et al. 2013] at approximately 1° horizontal resolution in all model components. Like most state-of-the-art global coupled climate models, CESM1(CAM5) consists of coupled atmosphere, ocean, land, and sea ice component models (Fig. 1). In addition to land carbon cycle calculations, the CESM-LE simulations also include diagnostic biogeochemistry calculations for the ocean ecosystem and the atmospheric carbon dioxide cycle (Lawrence et al. 2012; Long et al. 2013; Moore et al. 2013; Lindsay et al. 2014). Unlike the land carbon cycle calculations, which affect local energy and water cycles, the ocean biogeochemistry and atmospheric carbon dioxide tracer calculations do not affect the climate of the CESM-LE simulations. Many aspects of fully coupled simulations performed with CESM1(CAM5) are documented in a special collection of the *Journal of Climate* (see http://journals.ametsoc.org/page/CCSM4/CESM1).

We began the CESM-LE with a multicentury 1850 control simulation with constant preindustrial forcing (Table 1; Fig. 2). While the ocean model was initialized from observations, the atmosphere, land, and sea ice models were initialized using previous CESM1(CAM5) simulations. Atmosphere, land, and sea ice processes have memory on short time scales (weeks to years), so the influence of their initial conditions on the coupled climate state in a multicentury-long control simulation is negligible. In contrast, the ocean has memory on long time scales (up to several thousand years in the abyssal ocean). As a result, ocean initial conditions can influence multicentury coupled climate model runs. Because global ocean observations are not available for 1850, we initialized the ocean from a state of rest (Danabasoglu et al. 2012) using modern observations. Specifically, we initialized the ocean model with January mean climatological Polar Science Center Hydrographic Climatology (PHC2)

Table 1. CESM-LE simulations. Additional information about the simulations including all of the saved variables, diagnostics, model support, and known issues can be found at the CESM-LE web page (www2.cesm.ucar.edu/models/experiments/LENS).

	1850 fully coupled control	1850 atmosphere and land control	Ensemble member 1	Ensemble member 2–*N*
Case name[a]	b.e11.B1850C5CN.f09_g16.005	f.e11.F1850C5CN.f09_f09.001	b.e11.B20TRC5CNBDRD.f09_g16.001, b.e11.BRCP85C5CNBDRD.f09_g16.001	b.e11.B20TRC5CNBDRD.f09_g16.00N, b.e11.BRCP85C5CNBDRD.f09_g16.00N
Years[b]	1,500 years, years 400–1500 released	2,000 years, years 1–1999 released	1850–2100	1920–2100
Prognostic model components	Atmosphere, ocean, land, sea ice	Atmosphere, land	Atmosphere, ocean, land, sea ice	Atmosphere, ocean, land, sea ice
Forcing	Preindustrial (1850), Whole Atmosphere Community Climate Model (WACCM) ozone forcing[c]	Preindustrial (1850) with prescribed monthly mean sea surface temperature and sea ice averaged over years 402–1510 of the 1850 control, WACCM ozone forcing[c]	1850–2005 historical, 2006–2100 RCP8.5 well-mixed greenhouse gases (Meinshausen et al. 2011) and short-lived gases and aerosols (Lamarque et al. 2011), WACCM ozone forcing[c]	Same as ensemble member 1 for overlapping years
Initialization	Jan mean present-day potential temperature and salinity from PHC2 dataset for ocean, previous CESM1(CAM5) 1850 control run for atmosphere, land, and sea ice	1 Jan, year 402 of 1850 coupled control for atmosphere and land. For ocean/ice, N/A.	1 Jan, year 402 of 1850 coupled control for all model components (atmosphere, land, ocean, sea ice)	Ensemble member 2: 1 Jan 1920 of ensemble member 1 started with 1-day lagged ocean temperatures
				Ensemble members 3–*N*: 1 Jan 1920 of ensemble member 1 for all model components; atmosphere with round-off (order of 10^{-14} K) differences in air temperature

[a] Simulation output using the case names listed in this table are available to download from the ESG (www.earthsystemgrid.org).

[b] Simulations may be extended and additional years will be posted on the ESG.

[c] We elected to use ozone concentrations produced by CESM1(WACCM) for the CESM-LE because the CMIP5 CESM ozone forcing underestimates the strength of stratospheric ozone depletion over Antarctica (Eyring et al. 2013). Indeed, the ozone hole is more pronounced, realistic, and internally consistent in CESM1(WACCM) than it is in the CESM CMIP5 simulations. The CESM-LE 1850 control run was forced by the average seasonal cycle of ozone concentrations from 200 years of a CESM1(WACCM) 1850 control run. For the transient ensemble members, WACCM ozone concentrations were taken from available CESM1(WACCM) CMIP5 simulations (average of two ensemble members for 1955–2055, single ensemble member for 1850–1954 and 2056–2100). Following CMIP5 external forcing protocol, we wanted the applied WACCM ozone forcing to emphasize externally forced ozone variations and deemphasize internal climate variability in the CESM1(WACM) CMIP5 simulations. As such, we applied a 10-yr running mean to each month of ozone forcing separately. This smoothing reduces the impact of CESM1(WACM)-specific internal climate variability (e.g., ENSO variability and sudden stratospheric warmings) on the ozone concentrations that are applied to the CESM-LE. The smoothing also minimizes the impact of the 11-yr solar cycle on stratospheric ozone concentrations.

Table 2. CMIP5 models and expansions.	
Model name	Model expansion
ACCESS1.0	Australian Community Climate and Earth-System Simulator, version 1.0
ACCESS1.3	Australian Community Climate and Earth-System Simulator, version 1.3
BCC_CSM1.1	Beijing Climate Center, Climate System Model, version 1.1
BCC_CSM1.1(m)	Beijing Climate Center, Climate System Model, version 1.1 (moderate resolution)
BNU-ESM	Beijing Normal University–Earth System Model
CanESM2	Second Generation Canadian Earth System Model
CCSM4	Community Climate System Model, version 4
CESM1(BGC)	Community Earth System Model, version 1 (biogeochemical)
CESM1(CAM5)	Community Earth System Model, version 1 (Community Atmosphere Model, version 5)
CESM1(WACCM)	Community Earth System Model, version 1 (Whole Atmosphere Community Climate Model)
CMCC-CMS	Centro Euro-Mediterraneo per I Cambiamenti Climatici Stratosphere-resolving Climate Model
CNRM-CM5	Centre National de Recherches Météorologiques Coupled Global Climate Model, version 5
CSIRO-Mk3.6.0	Commonwealth Scientific and Industrial Research Organisation Mark 3.6.0
EC-EARTH	European Consortium Earth System Model
FGOALS-g2	Flexible Global Ocean–Atmosphere–Land System Model gridpoint, version 2.0
FIO-ESM	First Institute of Oceanography (FIO) Earth System Model (ESM)
GFDL-CM3	Geophysical Fluid Dynamics Laboratory Climate Model, version 3
GFDL-ESM2G	Geophysical Fluid Dynamics Laboratory Earth System Model with Generalized Ocean Layer Dynamics (GOLD) component
GFDL-ESM2M	Geophysical Fluid Dynamics Laboratory Earth System Model with Modular Ocean Model (MOM), version 4, component
GISS-E2H	Goddard Institute for Space Studies Model E, coupled with the Hybrid Coordinate Ocean Model (HYCOM) ocean model
GISS-E2-H-CC	Goddard Institute for Space Studies Model E2, coupled with HYCOM and interactive terrestrial carbon cycle (and oceanic biogeochemistry)
GISS-E2-R	Goddard Institute for Space Studies Model E2, coupled with the Russell ocean model
GISS-E2-R-CC	Goddard Institute for Space Studies Model E2, coupled with Russell and interactive terrestrial carbon cycle (and oceanic biogeochemistry)
HadGEM2-AO	Hadley Centre Global Environment Model, version 2—Atmosphere and Ocean
HadGEM2-ES	Hadley Centre Global Environment Model, version 2—Earth System
INM-CM4.0	Institute of Numerical Mathematics Coupled Model, version 4.0
INGV-SXG	Istituto Nazionale di Geofisica e Vulcanologia, SINTEX-G
IPSL-CM4	L'Institut Pierre-Simon Laplace Coupled Model, version 4
IPSL-CM5A-LR	L'Institut Pierre-Simon Laplace Coupled Model, version 5A, low resolution
IPSL-CM5A-MR	L'Institut Pierre-Simon Laplace Coupled Model, version 5A, mid resolution
IPSL-CM5B-LR	L'Institut Pierre-Simon Laplace Coupled Model, version 5B, low resolution
MIROC5	Model for Interdisciplinary Research on Climate, version 5
MIROC-ESM	Model for Interdisciplinary Research on Climate, Earth System Model
MIROC-ESM-CHEM	Model for Interdisciplinary Research on Climate, Earth System Model, Chemistry Coupled
MPI-ESM-LR	Max Planck Institute Earth System Model, low resolution
MRI-CGCM3	Meteorological Research Institute Coupled Atmosphere–Ocean GCM, version 3
NorESM1-M	Norwegian Earth System Model, version 1 (intermediate resolution)
NorESM1-ME	NorESM1-M with carbon cycling (and biogeochemistry)

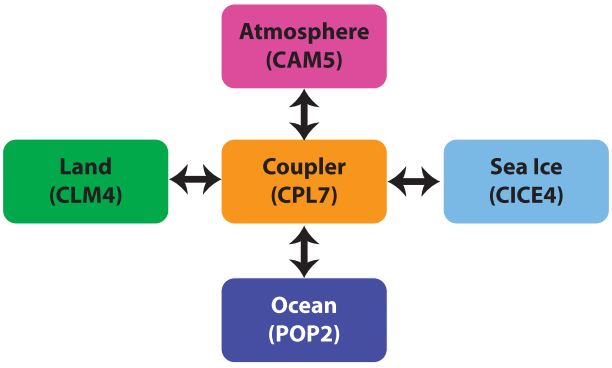

Fig. 1. CESM1(CAM5) component models and coupling (Hurrell et al. 2013). All components were run at ~1° horizontal resolution. CESM1(CAM5) consists of coupled atmosphere (CAM5, 30 vertical levels), ocean [Parallel Ocean Program, version 2 (POP), 60 vertical levels], land [Community Land Model, version 4 (CLM4)], and sea ice [Los Alamos Sea Ice Model (CICE)] component models.

potential temperature and salinity data. The PHC2 dataset represents a blending of the Levitus et al. (1998) with Steele et al. (2001) data for the Arctic Ocean. Ocean biogeochemical tracers were initialized from a separate 600-yr spinup.

Our 1850 ocean initialization strategy leverages two assumptions. First, the upper ocean equilibrates on much shorter time scales than the deep ocean. Therefore, the upper ocean adjusts to a preindustrial state after several decades under constant forcing. Second, modern observations still reflect preindustrial conditions at depth because of the long abyssal ocean equilibrium time scales. After an expected initial surface ocean cooling, the 1850 control arrived at a balanced coupled state with climate drift only in the deep ocean (global ocean temperature drift of ~0.005 K century^{-1} for years 400–1000).

After a few centuries, the control run climate was in quasi equilibrium with the 1850 forcing. At this point, we started the first ensemble member using initial conditions from a randomly selected date in the 1850 control run: 1 January, year 402 (Table 1). Ensemble member 1 was integrated forward from 1850 to 2100 (Fig. 2). Ensemble members 2–30 were all started on 1 January 1920 using slightly different initial conditions (Table 1). Spread in ensemble members 3–30 was generated by round-off level differences in their initial air temperature fields. Specifically, we applied random round-off level (order of 10^{-14} K) differences to the air temperature field of ensemble member 1 to generate atmospheric initial conditions for ensemble members 3–30. With the exception of their initial air temperature field, ensemble members 3–30 all had the same initial conditions. For technical reasons, ensemble member 2 was started using a 1-day lagged ocean initial condition. Because all 30 CESM-LE members share essentially the same ocean initial conditions, the CESM-LE does not sample internal climate variability resulting from differing ocean states.

All CESM-LE ensemble members have the same specified external forcing. Following the CMIP5 design protocol, we applied historical forcing from 1920 to 2005 (Lamarque et al. 2010) and representative concentration pathway 8.5 (RCP8.5) forcing (Meinshausen et al. 2011; Lamarque et al. 2011) from 2006 to 2100. Unlike the CMIP5 CESM runs, which specified ozone forcing from the CAM-Chem model ("CMIP5 CESM ozone"; Lamarque et al. 2010, 2011; Meehl et al. 2012), the CESM-LE simulations use ozone concentrations calculated by a high-top coupled chemistry–climate model {CESM1[Whole Atmosphere Community Climate Model (WACCM)]; Marsh et al. 2013} with specified ozone depleting substances (Table 1).

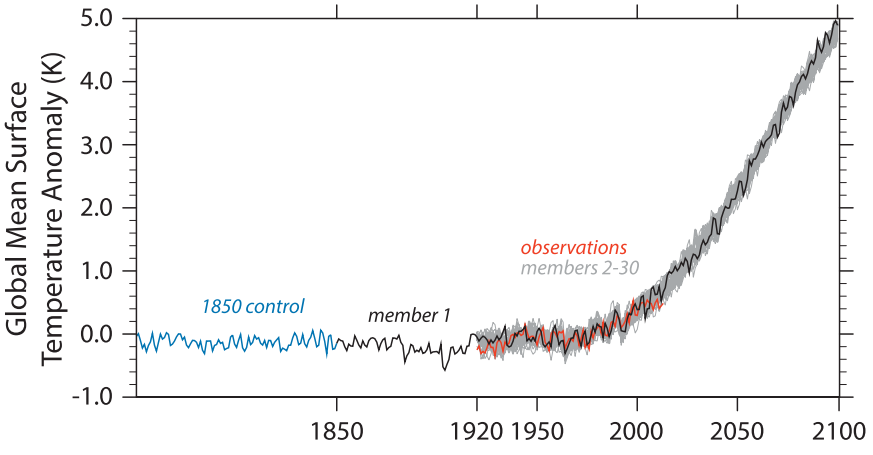

Fig. 2. Global surface temperature anomaly (1961–90 base period) for the 1850 control, individual ensemble members, and observations (HadCRUT4; Morice et al. 2012).

In response to the applied historical and RCP8.5 external forcing from 1920 to 2100, the global surface temperature increases by approximately 5 K in all ensemble members (Fig. 2). This consistent ~5-K global warming signal in all ensemble members by year 2100 reflects the climate response to forcing and

feedback processes as represented by this particular climate model. In contrast, internal variability causes a relatively modest 0.4-K spread in warming across ensemble members. The global surface air temperature evolution in the CESM-LE simulations is similar to that in CMIP5 CESM1(CAM5) experiments contributed to CMIP5 (Meehl et al. 2013).

Completing the CESM-LE simulations required substantial computational, storage, and human resources. The CESM-LE is a "big data" project for the current generation of computing. All CESM-LE simulations were run on Yellowstone, NCAR's high-performance computing resource. Each CESM-LE member (1920–2100) took ~3 weeks to complete and produced 6.6 TB (15.3 TB) of postprocessed (raw) output. When combined with the preindustrial controls, a total of over 17 million Yellowstone core hours in over 1,500 individual jobs were required to complete the CESM-LE simulations. The total postprocessed archived data volume for the CESM-LE simulations (200+ TB) exceeds the entire CESM contribution to CMIP5 (~170 TB).

The CESM-LE outputs are publicly available via the Earth System Grid (ESG; www.earthsystemgrid.org) as single-variable time series in self-documenting lossless compressed netCDF-4 format. All saved outputs—including variable names, units, and frequency—are detailed on the CESM-LE website. A unique aspect of the CESM-LE is the large number of high-frequency fields that have been saved. Continuous daily outputs will be useful for studying extremes on socially relevant time scales. The 6-hourly outputs during three 10-yr periods (1996–2005, 2025–34, and 2071–80) enable cyclone tracking and can serve as boundary conditions for regional climate model simulations, among other applications. Of interest to those planning offshoot experiments, the files required to restart CESM are saved every five years in all ensemble members. The experimental design for the CESM-LE project is reproducible. The code base and associated external forcing files are also available on the Earth System Grid.

ILLUSTRATIVE RESULTS AND THE QUESTIONS THEY INSPIRE. With the ensemble experimental design described, we next present thought-provoking initial results from the CESM-LE. We begin with global-mean surface air temperature trends. Global-mean trends are less affected by internal climate variability than regional trends. Yet, the influence of internal climate variability on global trends has recently emerged as an important research topic because of the observed global surface warming "hiatus" or the reduction in the rate of global surface air temperature increase since the mid-1990s (Tollefson 2014; see Fig. 2).

One leading hypothesis for the global warming hiatus implicates internally generated, deep ocean heat uptake. While the surface ocean cools, the deep ocean traps heat and thus warming decelerates (Meehl et al. 2011; Kosaka and Xie 2013; Trenberth and Fasullo 2013; England et al. 2014; Clement and Dinezio 2014). Another hypothesis posits that increased stratospheric aerosol from volcanic eruptions contributes to the hiatus (Solomon et al. 2011; Neely et al. 2013; Santer et al. 2014). The CESM-LE can help address the causes of global surface warming acceleration and deceleration. For example, how do modes of coupled internal climate variability and external forcing jointly affect global warming trends, and what mechanisms are involved?

To illustrate the influence of internal climate variability on global warming trends in the CESM-LE, Fig. 3 shows histograms of 10- and 20-yr global surface air temperature trends for the preindustrial (1850), the present (1990–2009), and the near future (2030–49). The preindustrial control run has constant 1850 forcing, a balanced top-of-atmosphere energy budget, and negligible climate drift. As a result, the 10- and 20-yr preindustrial trend histograms are symmetric about 0 (no trend). Even with a stable mean climate, there is a range in preindustrial trend magnitudes (e.g., −0.2 to +0.2 K decade^{-1} for 20-yr trends). This range is a measure of unforced internally generated climate variability, and the size of this range depends on the length of the interval over which trends are computed (e.g., Hunt and Elliot 2006). For example, the largest 10-yr trends are approximately twice the magnitude of the largest 20-yr trends.

By the late twentieth century/early twenty-first century, global warming has occurred in all ensemble members (Fig. 2), and the majority of the 10-yr and all of the 20-yr trends are positive (Fig. 3). Like the preindustrial, there is a considerable range of warming rates because of the internal climate variability. Of interest to hiatus research, recently observed 10- and 20-yr global surface air temperature trends are within the trend spread predicted by the CESM-LE ensemble members. In other words, the observed global warming hiatus is within the lower end of the range of plausible global warming responses to historical forcing as predicted by this particular climate model. Looking to the future, cooling trends become increasingly unlikely. Indeed, while a range in trend magnitude remains, 10- and 20-yr cooling trends no longer occur in the mid-twenty-first century under RCP8.5 forcing. In summary, initial analysis of the

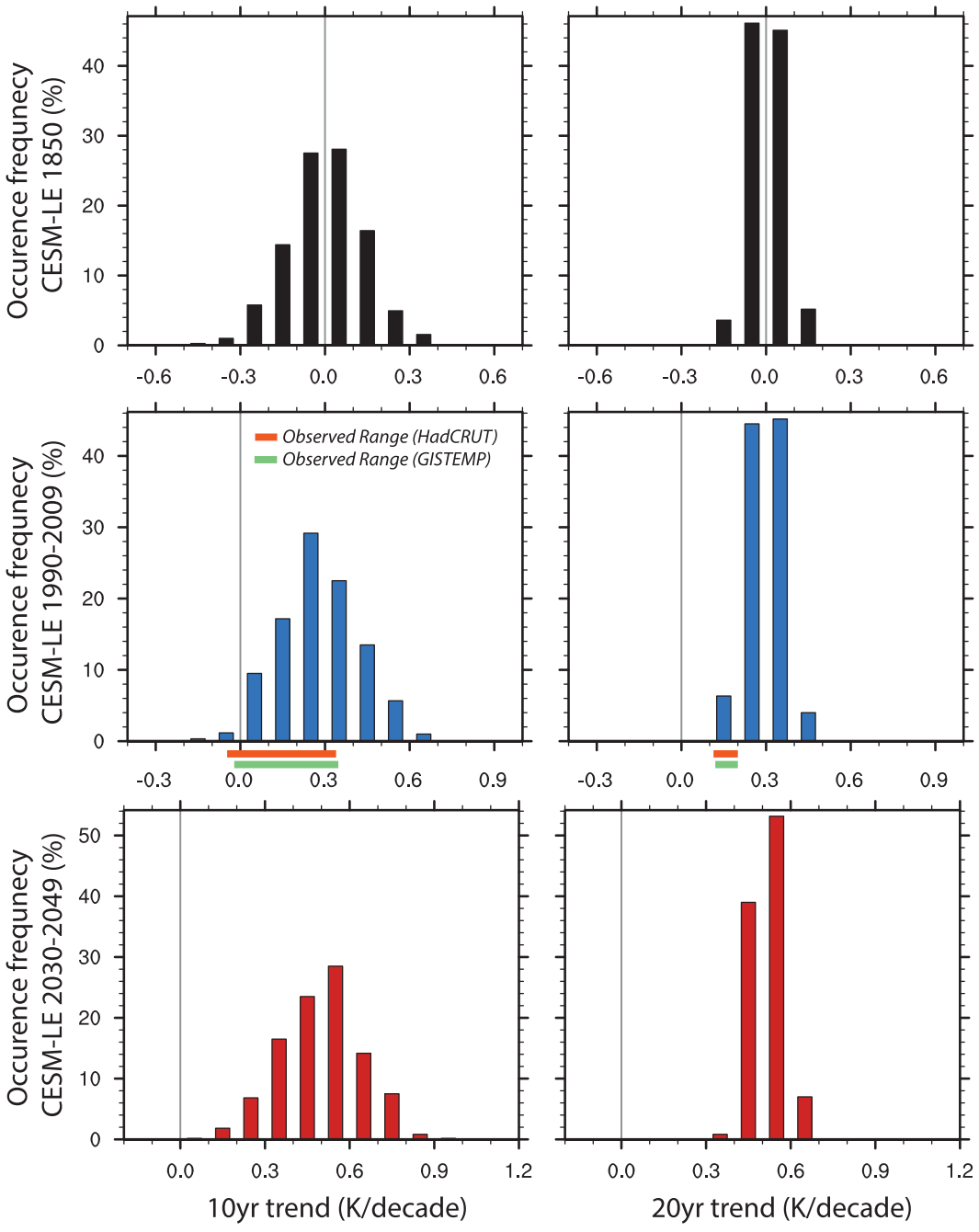

FIG. 3. Histograms of 10- and 20-yr trends in global surface air temperature for the 1850 control (black), starting from 1990 to 2009 (blue) and starting from 2030 to 2049 (red). Trends were calculated using time series of monthly mean values. The number of trends contributing to each histogram is not identical. For the 1850 control, independent continuous 10- and 20-yr segments were used to calculate trends. For the 1990–2009 and 2030–49 periods, trends were calculated for every possible start year. For example, for the period 1990–2009, 10-yr trends were calculated using Jan 1990–Dec 1999, Jan 1991–Dec 2000, … , Jan 2009–Dec 2018, while the 20-yr trends were calculated as Jan 1990–Dec 2009, Jan 1991–Dec 2010, … , Jan 2009–Dec 2028. Observed ranges are from HadCRUT4 (Morice et al. 2012) and Goddard Institute for Space Studies Surface Temperature Analysis (GISTEMP; Hansen et al. 2010). Observed trend minimum–maximum ranges were based on 10-yr trends calculated from Jan 1990–Dec 1999, Jan 1991–Dec 2000, … , Jan 1994–Dec 2013 and on 20-yr trends calculated from Jan 1990–Dec 2009, Jan 1991–Dec 2010, … , Jan 1994–Dec 2013.

CESM-LE global temperature trends supports existing research showing that global-mean surface air temperatures can show no trend or even slight cooling in the presence of long-term warming (e.g., Easterling and Wehner 2009), but unlike previous studies based on ensembles of opportunity that mix together climate model differences and internal variability, the CESM-LE shows that internal variability alone can generate substantial spread in global warming trends.

Having shown that internal climate variability can exert a substantial influence on global-mean temperature trends, we next look regionally, where we expect the influence of internal climate variability to be even larger. In particular, we use trend maps to illustrate the "single realization problem," the fact that any individual climate trajectory deviates from the mean forced response (e.g., Bengtsson et al. 2006; Easterling and Wehner 2009). Figure 4 shows boreal winter [December–February (DJF)] surface air temperature trends over the era with the best global observational coverage (1979–2012). The ensemble mean, an estimate of the forced response, depicts the familiar patterns of Arctic amplification and more warming over land than over the ocean. While the ensemble mean is useful for identifying the forced climate response, comparing across the individual ensemble members illustrates that the forced response is rarely realized. Why? The CESM-LE members show that regional trends can vary dramatically in magnitude and sign because of the internal climate variability. For example, the East Coast of the United States warms by about 3 K over the period 1979–2012 in ensemble member 6 but cools by about 3 K over the same period in ensemble member 13. Similarly, much of Eurasia cools by nearly 2 K in member 7, while the same region warms by about 3 K in member 17. The difference between ensemble member 6 and 13, and between 7 and 17, is the result of internal climate variability that cannot be predicted from initial condition differences at 1920.

Like any individual model ensemble member, the observations also represent one possible response of the climate system to external forcing in the presence of internal climate variability. As a consequence, comparing trends from a single ensemble member to the observed 1979–2012 temperature trends to "validate" the climate model simulation is problematic. Similarly problematic is comparing the ensemble-mean trend to observations, as internal climate variability is (by construction) muted in the ensemble mean. To confound matters even further, the available observations in some regions are too sparse to reliably detect a trend from observations alone [e.g., mountainous and polar regions in the Hadley Centre Climatic Research Unit temperature (HadCRUT4) dataset (Morice et al. 2012)].

When no ensemble member is able to reproduce the observed trend or when the trends in all ensemble members look more similar to each other than they do to the observed trend, the question becomes have we detected a model bias or have we inadequately sampled the ensemble spread? For example, none of the CESM-LE ensemble members replicate the magnitude of the observed surface cooling in the Southern Ocean or the eastern tropical Pacific over recent decades. For the Southern Ocean, the lack of surface cooling trends in the CESM-LE is consistent with associated weak ocean heat uptake in CESM1(CAM5). For the eastern tropical Pacific, the lack of pronounced surface cooling in the CESM-LE is directly relevant to hiatus research. Namely, the inability of any ensemble member to replicate the observed magnitude of the tropical Pacific Ocean surface cooling suggests that the tropical Pacific Ocean hypothesis [i.e., as tested by Kosaka and Xie (2013)] is not the only mechanism contributing to decelerated warming rates in the CESM-LE.

While the comparison of models and observations provides important insights, climate change projections are made in part to plan for a future we cannot observe. As such, we next examine the influence of internal climate variability on near-future trends, looking forward as far as we looked backward (i.e., 34 yr). Similar to Fig. 4, Fig. 5 shows that most CESM-LE members exhibit 2013–46 warming trends in most regions, with the exception of the North Atlantic. Yet, in some ensemble members, the internal climate variability is large enough to overwhelm the forcing and result in cooling in some regions. For example, ensemble member 20 shows pronounced cooling of 3 K over Asia that is in stark contrast to the appreciable warming of 6 K in that same region in ensemble member 24. The take-home message is clear, consistent with previous studies analyzing large ensembles with the same model and the same external forcing, and needs to be better communicated (e.g., Deser et al. 2012a): we need to plan for a range of future outcomes not only because climate models imperfectly represent the relevant processes, but also because there are inherent predictability limits in a climate system with large internal climate variability.

COMPARISON TO CMIP5. CMIP5 is frequently used to assess uncertainty in future climate projections. But CMIP5 is an ensemble of opportunity, and the spread within the CMIP5 archive is not easy to interpret. Individual CMIP5 ensemble members can have differing physics, dynamical cores, resolutions,

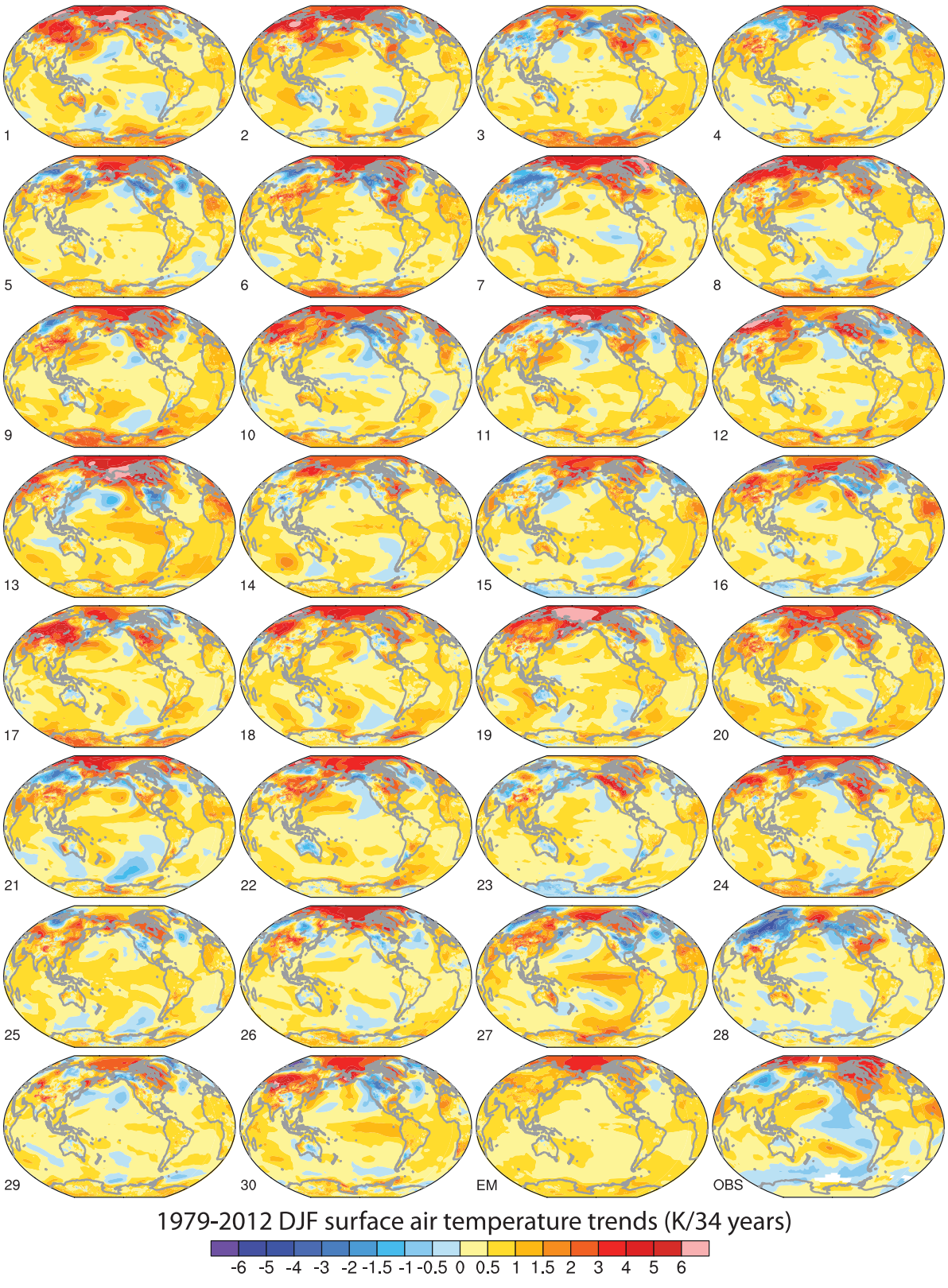

Fig. 4. Global maps of historical (1979–2012) boreal winter (DJF) surface air temperature trends for each of the 30 individual CESM-LE members, the CESM-LE ensemble mean (denoted EM), and observations (denoted OBS based on GISTEMP; Hansen et al. 2010).

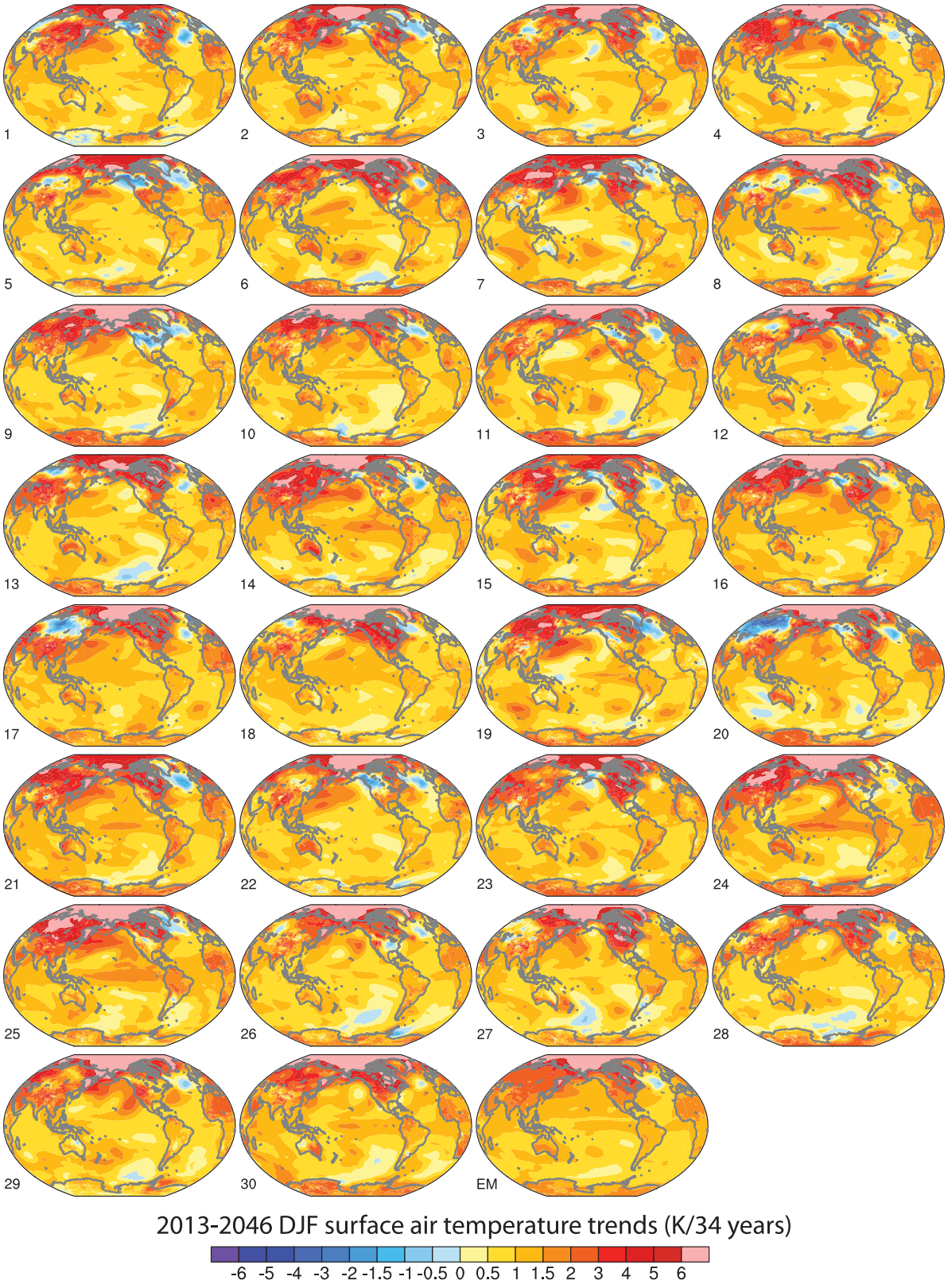

Fig. 5. Global maps of near-future (2013–46) boreal winter (DJF) surface air temperature trends for each of the 30 individual CESM-LE members and the CESM-LE ensemble mean (denoted EM).

and initial conditions. To complicate matters, many CMIP5 models share genes and are therefore not independent (Knutti et al. 2013). In sum, spread in CMIP5 climate projections results both from model formulation differences and from internal climate variability, the relative importance of which is unknown. Unlike the CMIP5 ensemble spread, CESM-LE ensemble spread is generated by internal climate variability alone. Given these points, a natural question becomes how much of the spread in CMIP5 projections can be explained by internal climate variability alone? We can answer this question by using the CESM-LE to estimate the influence of internal climate variability on ensemble spread.

Figure 6 shows spread in DJF surface air temperature trends during the preindustrial, historical, and near-future periods. We quantify spread for both the CESM-LE and CMIP5 using the standard deviation in 34-yr trends. Surprisingly, similar trend spread patterns and magnitudes are evident in the CESM-LE regardless of the time period selected. Reinforcing the visual similarity of the CESM-LE trend variability in all three periods (1850, 1979–2012, and 2013–46), statistically different trend variability is rare (i.e., few regions are stippled in the CESM-LE panels in Fig. 6). These comparisons suggest that internal climate variability in this particular variable and time span is largely independent of forcing. In other words, the influence of forced climate change on internal climate variability in 34-yr DJF surface air temperature is small. This result has practical relevance. Indeed, when internal climate variability does not change under climate forcing, long control runs and large forced ensembles will provide similar estimates of internal climate variability. Of even greater interest in Fig. 6, the trend spread generated by internal climate variability alone—estimated using the CESM-LE—is often statistically indistinguishable from the spread in trends within CMIP5. At least for DJF surface air temperature trends, the conclusion is stunning: CMIP5 spread in many regions (i.e., regions that are not stippled in the CMIP5 panels in Fig. 6) can be explained by internal climate variability [as estimated by CESM(CAM5)] alone.

While the trend variability comparisons in Fig. 6 are interesting, the implications are not universal. The contribution of internal climate variability to ensemble spread depends on the climate variable, time period, season, and location (e.g., Deser et al. 2012b). What is the relative contribution of model formulation differences and internal climate variability to changes in other climate variables? Why are there differences across climate variables, time periods, seasons, and locations? Where should we expect improved model formulations to reduce spread in future climate projections? These are the types of important climate questions that can be addressed by comparing CESM-LE and CMIP5 ensemble spread.

EXTREMES. Understanding extreme climate phenomena requires multiple realizations for adequate statistical sampling. To illustrate the utility of the CESM-LE for studying extreme climate phenomena, we next focus on detecting changes in the climatologies of extreme events. In particular, we analyze atmospheric blocking changes produced by differences in model physics and heat stress changes resulting from twenty-first-century RCP8.5 forcing.

Atmospheric blocking is often associated with extreme events in the midlatitudes. Under blocked atmospheric flow, persistent winter cold spells and summer heat waves occur. On the periphery of blocked regions, atypical weather patterns can also lead to surface temperature and precipitation extremes. Because blocking is a feature in the large-scale atmospheric flow, it is a relatively reliable proxy for extreme events in climate model simulations. Yet, blocking statistics have appreciable year-to-year variability and thus many years of data are needed to attribute changes in blocking statistics to model differences or to external forcing.

To illustrate the unique value of large ensembles for evaluating blocking climatologies, Fig. 7 compares Northern Hemisphere blocking frequency (D'Andrea et al. 1998) in the 30-member CESM-LE; a 30-member Community Climate System Model, version 4 (CCSM4) ensemble (Mudryk et al. 2014); and historical reanalysis. Substantial longitudinally dependent ensemble spread in climatological blocking frequency is evident in both 30-member ensembles, a finding that demonstrates the importance of large ensembles for evaluating mean state model blocking climatologies. Comparing the 30-member CCSM4 ensemble to the 30-member CESM-LE, we can confidently attribute blocking statistics differences to model physics differences. Specifically, the CESM-LE exhibits increased and improved blocking frequency over the Atlantic (30°W–15°E) when compared to CCSM4. Interestingly, the ensemble spread in the CESM-LE is greater than that in the CCSM4 ensemble over the eastern Atlantic (0°–30°E), hinting not only at differences in climatological-mean blocking but also in blocking variability.

Heat stress is a leading cause of weather-related human mortality and morbidity (Guirguis et al. 2014; CDC 2006). When the climate warms, heat stress

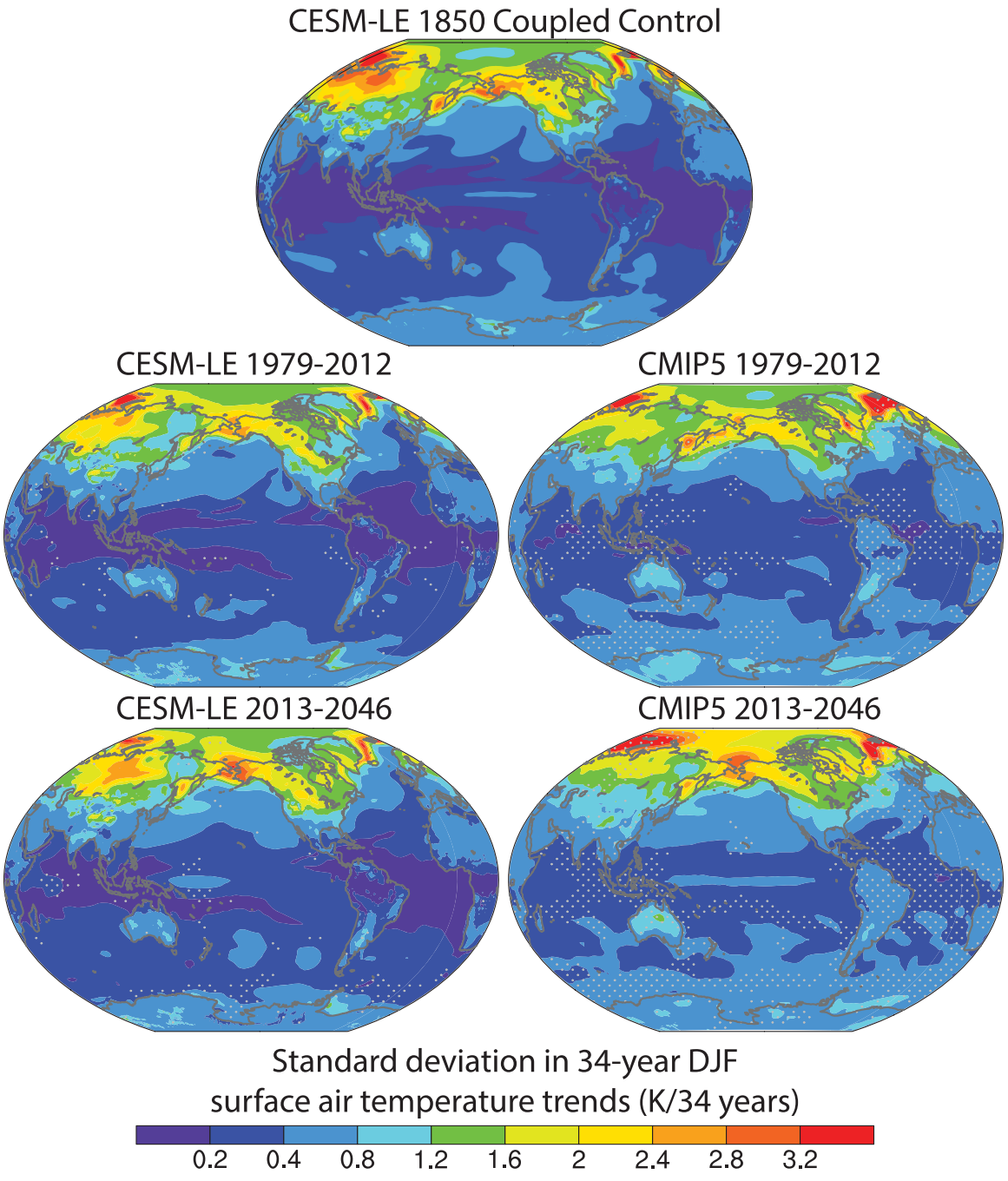

Fig. 6. Global maps of standard deviation in 34-yr DJF surface air temperature trends for the (top) preindustrial (1850), (middle) historical (1979–2012), and (bottom) near-future (2013–46) periods. For the historical and near-future periods, trends are shown for both the 30-member CESM-LE ensemble and the 38-member CMIP5 ensemble (Taylor et al. 2012). Stippling on the historical and near-future CESM-LE trend maps indicates standard deviations that are statistically different than the CESM-LE preindustrial period. Stippling on the historical and near-future CMIP5 maps indicates standard deviations that are statistically different than the CESM-LE for the corresponding period. Stippling is based on an *f* test and a 95% confidence interval. For CMIP5, we used a single (the first) ensemble member of the following models (see Table 2 for full list of expansions): ACCESS1.0, ACCESS1.3, BCC_CSM1.1(m), BCC_CSM1.1, BNU-ESM, CanESM2, CCSM4, CESM1(BGC), CESM1(CAM5), CESM1(WACCM), CMCC-CM, CMCC-CMS, CNRM-CM5, CSIRO Mk3.6.0, EC-EARTH, FGOALS-g2, FIO-ESM, GFDL CM3, GFDL-ESM2G, GFDL-ESM2M, GISS-E2-H, GISS-E2-H-CC, GISS-E2-R, GISS-E2-R-CC, HadGEM2-AO, HadGEM2-CC, HadGEM2-ES, INM-CM4.0, IPSL-CM5A-LR, IPSL-CM5A-MR, IPSL-CM5B-LR, MIROC5, MIROC-ESM, MIROC-ESM-CHEM, MPI-ESM-LR, MRI-CGCM3, NorESM1-M, and NorESM1-ME.

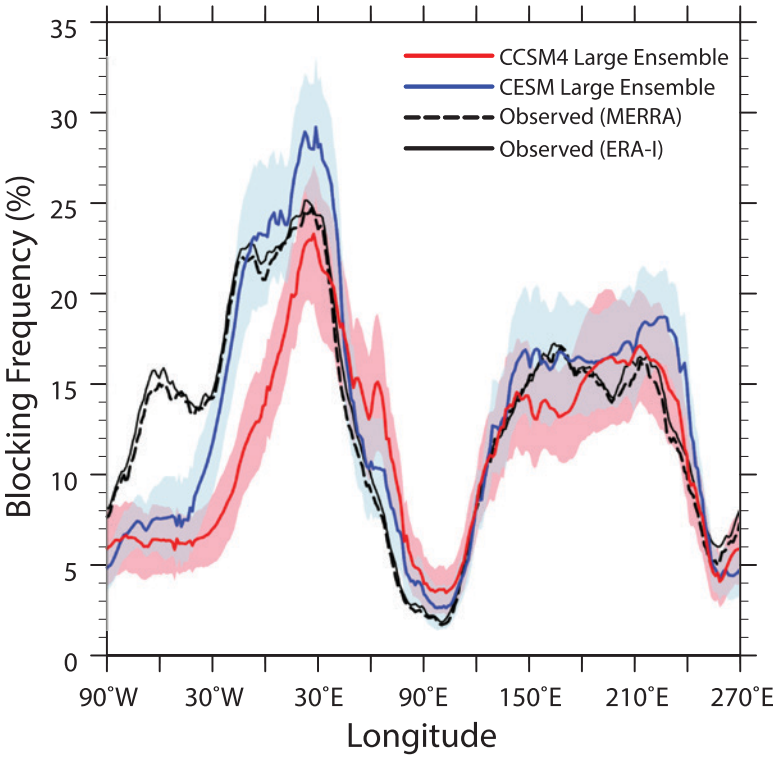

Fig. 7. Climatological meridional mean blocking frequency based on daily 500-mb geopotential height fields (D'Andrea et al. 1998) for 30 CESM-LE ensemble members, 30 CCSM4 ensemble members (Mudryk et al. 2014), and in observations [European Centre for Medium-Range Weather Forecasts (ECMWF) Interim Re-Analysis (ERA-Interim; Dee et al. 2011) and Modern-Era Retrospective Analysis for Research and Applications (MERRA; Rienecker et al. 2011) reanalysis] during boreal spring [March–May (MAM)]. Lines show mean values and shading shows plus or minus two standard deviation in the mean values. The periods are 1979–2010 (observations) and 1974–2005 (models). Note that differing periods were used for the models and observations, but blocking statistics are not affected by 5-yr differences in averaging intervals.

worsens in severity (e.g., hotter days and nights), frequency (number of hot days and nights), and duration (heat waves) (Meehl and Tebaldi 2004). At the same time, determining heat stress patterns and trends is not straightforward because of the wide variety of methodological approaches in defining a heat wave (Smith et al. 2013) and because of the internal climate variability (Perkins and Fischer 2013; Fischer et al. 2013). Daily outputs from the CESM-LE can be used to identify the mechanisms underlying regional differences in future heat stress projections (e.g., connection to atmospheric blocking or land–atmosphere feedbacks) and to assess the influence of internal climate variability on heat stress metrics. To illustrate the value of the large ensemble for the latter, Fig. 8 contrasts early twenty-first-century heat stress changes in all 30 CESM-LE members with corresponding changes in one randomly selected ensemble member (ensemble member 6). Over the early twenty-first century, heat wave intensity, duration, and frequency increase everywhere, but with regional magnitude differences. When all 30 ensemble members are used to detect heat stress changes, the results are statistically significant nearly everywhere. In contrast, the heat stress changes in ensemble member 6 are much less likely to be statistically significant and differ from the 30-member mean changes because of the unique expression of internal climate variability in this particular ensemble member.

NEW ANALYSES ENABLED. Reflecting the demand for an open-access large ensemble and community participation in the CESM-LE experimental design, analysis of CESM-LE simulations has already begun and interest is expected to grow. Using the CESM-LE framework, it is possible to cleanly separate forced climate change from internally generated variability, to quantify model projection spread, and to evaluate how variability coevolves with a changing climate. Research evaluating urban heat waves, atmospheric circulation and blocking, precipitation characteristics, snow cover, ozone hole impacts, air quality, Greenland Ice Sheet surface mass balance, sea ice, and hurricanes has already begun. Biogeochemical processes are being analyzed in a large ensemble framework for the first time including uptake and storage of anthropogenic carbon dioxide by the land and ocean, primary productivity by biology in the land and ocean, and variation of atmospheric carbon dioxide on seasonal to decadal time scales. Offshoot experiments have already started including experiments to test the competing hypotheses for hiatus periods, to evaluate hurricanes in CESM1(CAM5) using high-resolution time slice experiments, to force regional downscaling simulations, and to run a complementary ensemble under RCP4.5 forcing to assess avoided impacts. To help coordinate community analysis of the CESM-LE, we are compiling

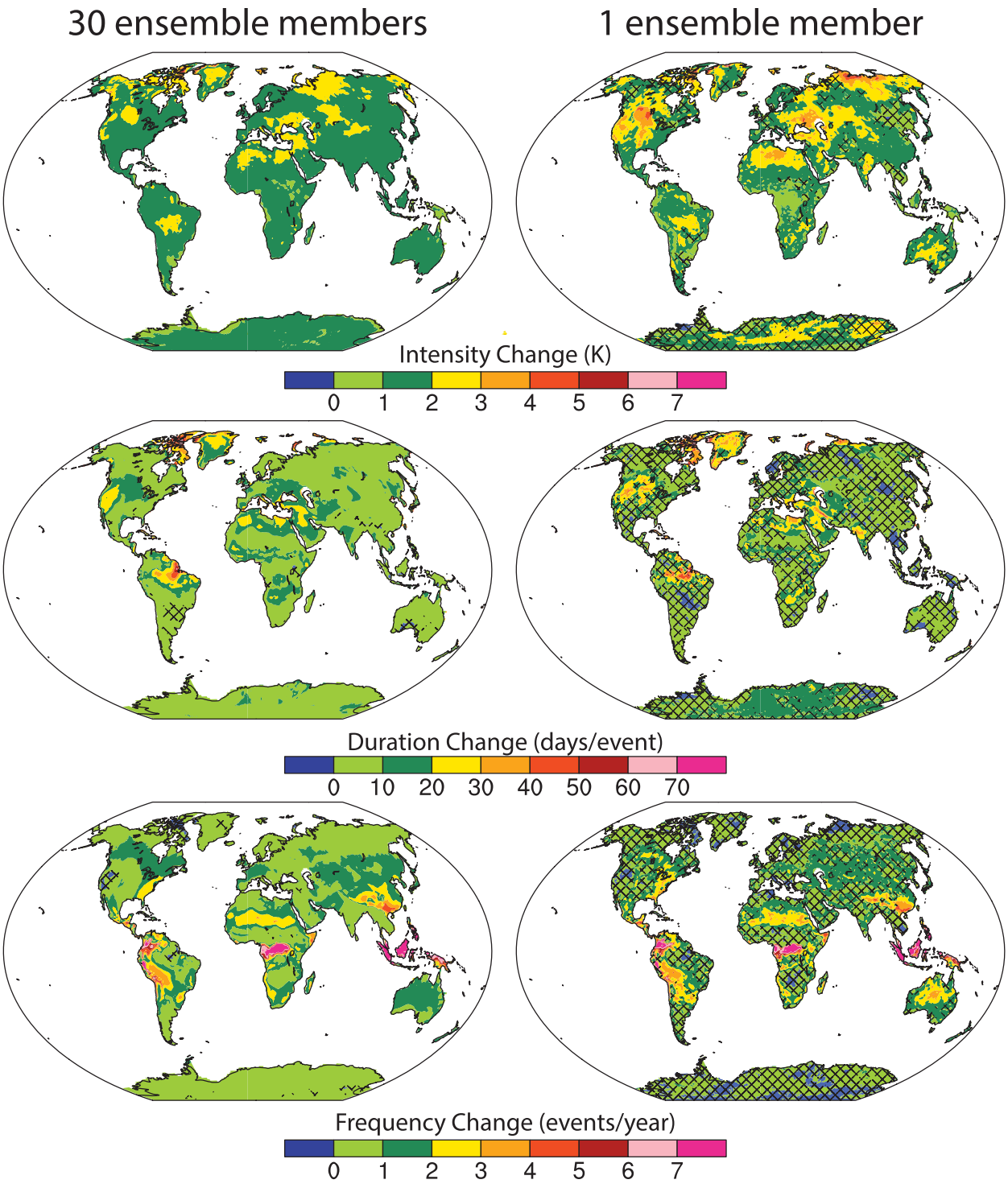

Fig. 8. Maps of early twenty-first-century change (2040s–2010s) in heatwave intensity, duration, and frequency from the CESM-LE for (left) 30 ensemble members and for (right) 1 ensemble member. Heat waves are defined following Meehl and Tebaldi (2004). Heat wave intensity, duration, and frequency were calculated for each year and then averaged. Hatching indicates differences are not statistically significant at the 95% level using a Student's *t* test.

a list of all ongoing projects at the CESM-LE website (www2.cesm.ucar.edu/models/experiments/LENS). A new resource useful for analyzing the CESM-LE, and for making comparisons to CMIP5, is the freely available Climate Variability Diagnostics Package (Phillips et al. 2014).

SUMMARY AND BROADER IMPLICATIONS. Understanding forced climate change in the presence of internal climate variability is a major challenge for climate prediction. To make progress, the science and stakeholder communities need relevant climate model experiments with useful outputs. The CESM-LE addresses this challenge through its transparent experimental design and relevant accessible outputs. Initial illustrative CESM-LE results affirm that because of the internal climate variability, single realizations from climate models are often insufficient for model comparison to the observational record, model intercomparison, and future projections. A publicly available ensemble with the scope, and the amount of community input as the CESM-LE, has never been performed before. We anticipate analysis of this ensemble, alone or in combination with other ensembles and/or regional climate simulations, will lead to novel and practical results that will inspire probabilistic thinking and inform planning for climate change and climate model development for many years to come.

ACKNOWLEDGMENTS. We thank the three reviewers who provided thoughtful comments and the scientists and software engineers that develop CESM and support Yellowstone. The National Science Foundation (NSF) and Regional and Global Climate Modeling Program (RGCM) of the U.S. Department of Energy's Office of Science (BER) support the CESM project. The NSF-sponsored Climate Simulation Laboratory at NCAR's Computational and Information Systems Laboratory (CISL) provided computing resources on Yellowstone.

REFERENCES

Bengtsson, L., K. I. Hodges, E. Roeckner, and R. Brokopf, 2006: On the natural variability of pre-industrial European climate. *Climate Dyn.,* **27,** 743–760, doi:10.1007/s00382-006-0168-y.

CDC, 2006: Heat-related deaths—United States, 1999–2003. Centers for Disease Control Mortality and Morbidity Weekly Rep. July 28, 2006/55(29), 796–798. [Available online at www.cdc.gov/mmwr/preview/mmwrhtml/mm5529a2.htm.]

Clement, A., and P. Dinezio, 2014: The tropical Pacific Ocean—Back in the driver's seat? *Science,* **343,** 976–978, doi:10.1126/science.1248115.

Danabasoglu, G., S. C. Bates, B. P. Briegleb, S. R. Jayne, M. Jochum, W. G. Large, S. Peacock, and S. G. Yeager, 2012: The CCSM4 ocean component. *J. Climate,* **25,** 1361–1389, doi:10.1175/JCLI-D-11-00091.1.

D'Andrea, F., and Coauthors, 1998: Northern Hemisphere atmospheric blocking as simulated by 15 atmospheric general circulation models in the period 1979–1988. *Climate Dyn.,* **14,** 385–407, doi:10.1007/s003820050230.

Dee, D. P., and Coauthors, 2011: The ERA-Interim reanalysis: Configuration and performance of the data assimilation system. *Quart. J. Roy. Meteor. Soc.,* **137,** 553–597, doi:10.1002/qj.828.

Deser, C., R. Knutti, S. Solomon, and A. S. Phillips, 2012a: Communication of the role of natural variability in future North American climate. *Nat. Climate Change,* **2,** 775–779, doi:10.1038/nclimate1562.

——, A. S. Phillips, V. Bourdette, and H. Teng, 2012b: Uncertainty in climate change projections: The role of internal variability. *Climate Dyn.,* **38,** 527–546, doi:10.1007/s00382-010-0977-x.

——, A. S. Phillips, M. A. Alexander, and B. V. Smoliak, 2014: Projecting North American climate over the next 50 years: Uncertainty due to internal variability. *J. Climate,* **27,** 2271–2296, doi:10.1175/JCLI-D-13-00451.1.

Easterling, D. R., and M. F. Wehner, 2009: Is the climate warming or cooling? *Geophys. Res. Lett.,* **36,** L08706, doi:10.1029/2009GL037810.

England, M. H., and Coauthors, 2014: Recent intensification of wind-driven circulation in the Pacific and the ongoing warming hiatus. *Nat. Climate Change,* **4,** 222–227, doi:10.1038/nclimate2106.

Eyring, V., and Coauthors, 2013: Long-term ozone changes and associated climate impacts in CMIP5 simulations. *J. Geophys. Res. Atmos.,* **18,** 5029–5060, doi:10.1002/jgrd.50316.

Fischer, E. M., U. Beyerle, and R. Knutti, 2013: Robust spatially aggregated projections of climate extremes. *Nat. Climate Change,* **3,** 1033–1038, doi:10.1038/nclimate2051.

Goddard, L., and Coauthors, 2013: A verification framework for interannual-to-decadal predictions experiments. *Climate Dyn.,* **40,** 245–272, doi:10.1007/s00382-012-1481-2.

Guirguis, K., A. Gershunov, A. Tardy, and R. Basu, 2014: The impact of recent heat waves on human health in California. *J. Appl. Meteor. Climatol.,* **53,** 3–19, doi:10.1175/JAMC-D-13-0130.1.

Hansen, J., R. Ruedy, M. Sato, and K. Lo, 2010: Global surface temperature change. *Rev. Geophys.,* **48,** RG4004, doi:10.1029/2010RG000345.

Hawkins, E., and R. Sutton, 2009: The potential to narrow uncertainty in regional climate predictions. *Bull. Amer. Meteor. Soc.,* **90,** 1095–1107, doi:10.1175/2009BAMS2607.1.

Hunt, B. G., and T. I. Elliot, 2006: Climatic trends. *Climate Dyn.,* **26,** 567–585, doi:10.1007/s00382-005-0102-8.

Hurrell, J., and Coauthors, 2013: The Community Earth System Model: A framework for collaborative research. *Bull. Amer. Meteor. Soc.,* **94,** 1339–1360, doi:10.1175/BAMS-D-12-00121.1.

Knutson, T. R., F. Zeng, and A. T. Wittenberg, 2013: Multimodel assessment of regional surface temperature trends: CMIP3 and CMIP5 twentieth-century simulations. *J. Climate,* **26,** 8709–8743, doi:10.1175/JCLI-D-12-00567.1.

Knutti, R., D. Masson, and A. Gettelman, 2013: Climate model genealogy: Generation CMIP5 and how we got there. *Geophys. Res. Lett.,* **40,** 1194–1199, doi:10.1002/grl.50256.

Kosaka, Y., and S.-P. Xie, 2013: Recent global-warming hiatus tied to equatorial Pacific surface cooling. *Nature,* **501,** 403–407, doi:10.1038/nature12534.

Lamarque, J. F., and Coauthors, 2010: Historical (1850–2000) gridded anthropogenic and biomass burning emissions of reactive gases and aerosols: Methodology and application. *Atmos. Chem. Phys.,* **10,** 7017–7039, doi:10.5194/acp-10-7017-2010.

——, and Coauthors, 2011: Global and regional evolution of short-lived radiatively-active gases and aerosols in the representative concentration pathways. *Climatic Change,* **109,** 191–212, doi:10.1007/s10584-011-0155-0.

Lawrence, D. M., K. W. Oleson, M. G. Flanner, C. G. Fletcher, P. J. Lawrence, S. Levis, S. C. Swenson, and G. B. Bonan, 2012: The CCSM4 land simulation, 1850–2005: Assessment of surface climate and new capabilities. *J. Climate,* **25,** 2240–2260, doi:10.1175/JCLI-D-11-00103.1.

Levitus, S., and Coauthors, 1998: *Introduction.* Vol. 1, *World Ocean Database 1998,* NOAA Atlas NESDIS 18, 346 pp.

Lindsay, K., and Coauthors, 2014: Preindustrial-control and twentieth-century carbon cycle experiments with the Earth system model CESM1(BGC). *J. Climate,* **27,** 8981–9005, doi:10.1175/JCLI-D-12-00565.1.

Long, M. C., K. Lindsay, S. Peacock, J. K. Moore, and S. C. Doney, 2013: Twentieth-century oceanic carbon uptake and storage in CESM1(BGC). *J. Climate,* **26,** 6775–6800, doi:10.1175/JCLI-D-12-00184.1.

Lorenz, E. N., 1963: Deterministic nonperiodic flow. *J. Atmos. Sci.,* **20,** 130–141, doi:10.1175/1520-0469(1963)020<0130:DNF>2.0.CO;2.

Marsh, D. R., M. J. Mills, D. E. Kinnison, J.-F. Lamarque, N. Calvo, and L. M. Polvani, 2013: Climate change from 1850 to 2005 simulated in CESM1(WACCM). *J. Climate,* **26,** 7372–7391, doi:10.1175/JCLI-D-12-00558.1.

Meehl, G. A., and C. Tebaldi, 2004: More intense, more frequent, and longer lasting heat waves in the 21st century. *Science,* **305,** 994–997, doi:10.1126/science.1098704.

——, J. M. Arblaster, J. T. Fasullo, A. Hu, and K. E. Trenberth, 2011: Model-based evidence of deep-ocean heat uptake during surface-temperature hiatus periods. *Nat. Climate Change,* **1,** 360–364, doi:10.1038/nclimate1229.

——, and Coauthors, 2012: Climate system response to external forcings and climate change projections in CCSM4. *J. Climate,* **25,** 3661–3683, doi:10.1175/JCLI-D-11-00240.1.

——, and Coauthors, 2013: Climate change projections in CESM1 (CAM5) compared to CCSM4. *J. Climate,* **26,** 6287–6308, doi:10.1175/JCLI-D-12-00572.1.

Meinshausen, M., and Coauthors, 2011: The RCP greenhouse gas concentrations and their extension from 1765 to 2300. *Climatic Change,* **109,** 213–241, doi:10.1007/s10584-011-0156-z.

Moore, J. K., K. Lindsay, S. C. Doney, M. C. Long, and K. Misumi, 2013: Marine ecosystem dynamics and biogeochemical cycling in the Community Earth System Model [CESM1(BGC)]: Comparison of the 1990s with the 2090s under the RCP4.5 and RCP8.5 scenarios. *J. Climate,* **26,** 9291–9312, doi:10.1175/JCLI-D-12-00566.1.

Morice, C. P., J. J. Kennedy, N. A. Rayner, and P. D. Jones, 2012: Quantifying uncertainties in global and regional temperature change using an ensemble of observational estimates: The HadCRUT4 data set. *J. Geophys. Res.,* **117,** D08101, doi:10.1029/2011JD017187.

Mudryk, L. R., P. J. Kushner, and C. Derksen, 2014: Interpreting observed Northern Hemisphere snow trends with large ensembles of climate simulations. *Climate Dyn.,* **43,** 345–359, doi:10.1007/s00382-013-1954-y.

Murphy, J. M., D. M. H. Sexton, D. N. Barnett, G. S. Jones, M. J. Webb, M. Collins, and D. A. Stainforth, 2004: Quantification of modelling uncertainties in a large ensemble of climate change simulations. *Nature,* **430,** 768–772, doi:10.1038/nature02771.

Neely, R. R., III, and Coauthors, 2013: Recent anthropogenic increases in SO_2 from Asia have minimal impact on stratospheric aerosol. *Geophys. Res. Lett.,* **40,** 999–1004, doi:10.1002/grl.50263.

Perkins, S. E., and E. M. Fischer, 2013: The usefulness of different realizations for the model evaluation of regional trends in heat waves. *Geophys. Res. Lett.,* **40,** 5793–5797, doi:10.1002/2013GL057833.

Phillips, A. S., C. Deser and J. Fasullo, 2014: Evaluating modes of variability in climate models. *Eos Trans. Amer. Geophys. Union,* **95,** 453–455.

Rienecker, M. M., and Coauthors, 2011: MERRA: NASA's Modern-Era Retrospective Analysis for Research and Applications. *J. Climate,* **24,** 3624–3648, doi:10.1175/JCLI-D-11-00015.1.

Roeckner, E., and Coauthors, 2003: The atmospheric general circulation model ECHAM5. Part I: Model description. Max-Planck-Institut für Meteorologie Rep. 349, 127 pp.

Santer, B., and Coauthors, 2014: Volcanic contribution to decadal changes in tropospheric temperature. *Nat. Geosci.,* **7,** 185–189, doi:10.1038/ngeo2098.

Smith, T. T., B. F. Zaitchik, and J. M. Gohlke, 2013: Heat waves in the United States: Definitions, patterns, and trends. *Climatic Change,* **118,** 811–825, doi:10.1007/s10584-012-0659-2.

Solomon, S., J. S. Daniel, R. R. Neely III, J.-P. Vernier, E. G. Dutton, and L. W. Thomason, 2011: The persistently variable "background" stratospheric aerosol layer and global climate change. *Science,* **333,** 866–870, doi:10.1126/science.1206027.

Steele, M., R. Morley, and W. Ermold, 2001: PHC: A global ocean hydrography with a high quality Arctic Ocean. *J. Climate,* **14,** 2079–2087, doi:10.1175/1520-0442(2001)014<2079:PAGOHW>2.0.CO;2.

Taylor, K. E., R. J. Stouffer, and G. A. Meehl, 2012: The CMIP5 experiment design. *Bull. Amer. Meteor. Soc.,* **93,** 485–498, doi:10.1175/BAMS-D-11-00094.1.

Tebaldi, C., J. M. Arblaster, and R. Knutti, 2011: Mapping model agreement on future climate projections. *Geophys. Res. Lett.,* **38,** L23701, doi:10.1029/2011GL049863.

Tollefson, J., 2014: The case of the missing heat. *Nature,* **505,** 276–278, doi:10.1038/505276a.

Trenberth, K. E., and J. T. Fasullo, 2013: An apparent hiatus in global warming? *Earth's Future,* **1,** 19–32, doi:10.1002/2013EF000165.

Science at Your Fingertips

AMS Journals are now optimized for viewing on your mobile device.

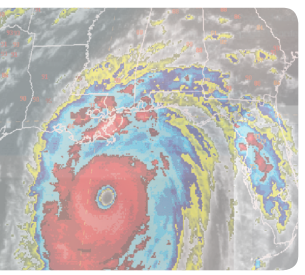

Access journal articles, monograph titles, and BAMS content using your iOS, Android, or Blackberry phone, or tablet.

Features include:

- **Saving articles for offline reading**
- **Sharing of article links via email and social networks**
- **Searching across journals, authors, and keywords**

And much more...

Scan code to connect to journals.ametsoc.org

AMERICAN METEOROLOGICAL SOCIETY